Available online at www.sciencedirect.com
SCIENCE DIRECT®
Advances in Space Research 33 (2004) 366–375
ADVANCES IN SPACE RESEARCH (a COSPAR publication)
www.elsevier.com/locate/asr

Shocks and particle acceleration in SNRs: theoretical aspects

A.M. Bykov

A.F.Ioffe Institute for Physics and Technology, St. Petersburg 194021, Russia

Received 2 December 2002; received in revised form 21 March 2003; accepted 21 April 2003

Abstract

Energetic particles are an essential component in supernova remnants (SNRs). Non-thermal particle acceleration in supernova shocks is expected to be an efficient process at different evolutional stages of SNRs. Non-linear wave–particle interactions being the governing process of the SNR collisionless shock formation are responsible for both shock heating and compression of the thermal gas as well as for creation of energetic particle population. The gas temperature behind such a shock could depart strongly from that predicted by the standard Rankine–Hugoniot law. We overview current models of collisionless supernova shocks with an emphasis on their confrontation with observed multi-wavelength spectra of SNRs from the radio to γ-rays. Simple scaling relations for post-shock ion temperature in the shocks with efficient particle acceleration are presented. A special attention is paid to the connections with high resolution SNR spectra currently obtained with XMM-Newton and Chandra. We discuss X-ray line emission from fast moving supernova ejecta fragments, arguing that they could contribute substantially to the observed line emission of the galactic ridge. We also consider the non-thermal appearance of SNRs interacting with molecular clouds.

Keywords: Shocks; Particle acceleration; Supernova remnants; Wave–particle interactions

1. Introduction: SNR collisionless shocks overview

The physical processes of relaxation of highly non-equilibrium flows of matter and energy released by a supernova (SN) explosion are of a fundamental importance in modeling the evolution of supernova remnants and studies of energy and chemical budgets of galaxies. Collisionless shock waves created after the explosive release of energy and matter are the main plasma heating agent and also serve as an universal source of energetic charged particles and radiation.

Modern high resolution SNR observations in radio, IR, optical, UV, and X-ray bands serve as probes to study the complex processes in the SNR shocks. Radio observations of electron synchrotron emission were the first clear sign of the presence of GeV regime relativistic electrons (positrons) in the shell-type SNRs. The relativistic particles are most probably related to the shock compression/acceleration processes.

Direct study of collisionless shock waves in laboratory is an extremely difficult task. Most of the experimental data on the collisionless shock physics are coming from space experiments. There are direct observational data on the shock wave structure in the interplanetary medium with clear evidences for ion and electron acceleration by the shocks (e.g., Tsurutani and Lin, 1985).

Computer simulations of the full structure of collisionless shock waves should describe the kinetics of multi-species particle flows and magneto-hydrodynamic (MHD) waves in the strongly coupled system. The problem is multi-scale. It requires a simultaneous treatment of both "microscopic" structure of a subshock at the thermal particle gyroradii scale where the injection process is thought to occur, and an extended "macroscopic" shock precursor due to energetic particles. The precursor scale is typically $\gg 10^6$ times of the microscopic scale of the subshock transition region.

Hybrid code modeling, that interprets protons as particles and electrons as a liquid, has made it possible to describe some important features of the (sub)shock waves on the microscopic scale. In the strong enough

E-mail address: byk@astro.ioffe.ru (A.M. Bykov).

0273-1177/$30 © 2003 COSPAR. Published by Elsevier Ltd. All rights reserved.
doi:10.1016/j.asr.2003.12.002

collisionless shocks (typically of a Mach number above a few) resistivity cannot provide energy dissipation fast enough to create a standard shock transition (e.g., Kennel et al., 1985) on a microscopic scale. Ion instabilities are important in such shocks that are called supercritical.

At the microscopic scale the front of a supercritical shock wave is a transition region occupied by magnetic field fluctuations of an amplitude $\delta B/B \sim 1$ and characteristic frequencies about the ion gyro-frequency. Generation of the fluctuations is due to instabilities in the interpenetrating multi-flow ion movements. The width of the transition region of a quasi-longitudinal shock wave reaches several dozen ion inertial lengths (defined as $l_{\rm i} = c/\omega_{\rm pi}$, where $\omega_{\rm pi}$ is the ion plasma frequency). The transition region of a quasi-perpendicular shock is somewhat narrower. The wave generation effects at the microscopic scale have been studied in some detail by hybrid code simulations (e.g., Krauss-Varban, 1995; Quest, 1988). The large-amplitude magnetic field fluctuation in the shock transition region was directly measured in the interplanetary medium (see e.g., Kan et al., 1991).

The reflected ions with a gyro-radius exceeding the width of the shock transition region can be then efficiently accelerated, via the Fermi mechanism, by converging plasma fluxes carrying MHD fluctuations. The efficiency of the upstream plasma flow energy conversion into non-thermal particles could be high enough providing a hard spectrum of non-thermal particles up to some maximal energy $\varepsilon_{\star}$. If the efficiency of ram energy transfer to the high energy particles is high enough, an extended shock precursor appears due to the incoming plasma flow deceleration by the fast particle pressure. The precursor scale is of the order of $(c/v_{\rm sh})\,\lambda_{\star}$ – orders of magnitude larger than the width of the shock transition region. Here, $\lambda_{\star}$ is the maximal mean free path of a particle in the energy-containing part of the spectrum and $v_{\rm sh}$ is the shock velocity.

The large scale (macroscopic) structure of the collisionless shock can be modeled by two-fluid approach with a kinetic description of non-thermal particles (see e.g., Blandford and Eichler, 1987; Malkov and Drury, 2001 for a review) or by a Monte Carlo method (e.g., Jones and Ellison, 1991). In both methods some suitable parameterization of particle scattering process must be postulated a priori. It has been shown that the front of a strong collisionless shock wave consists of an extended precursor and a viscous velocity discontinuity (subshock) of a local Mach number which is smaller than the total Mach number of the shock wave. The compression of matter at the subshock can be much lower than the total compression of the medium in the shock wave with allowance for high compression in the precursor. We shall refer such shocks later as CR-modified. Long before the first results describing the structure of a collisionless MHD shock wave modified by the pressure of cosmic ray (CR) particles were obtained, physical models of collisional shock waves were used in multi-liquid radiative gas dynamics. These models had predicted the structure of strong shock waves with a precursor.

Electron kinetics in collisionless shocks is very important because most of the observable emission comes from the electrons. Cargill and Papadopoulos (1988) modeled non-adiabatic electron heating in a strong quasi-transverse shock wave by the hybrid code method. The calculations showed the heating to be highly efficient. However, non-thermal electron distributions cannot be directly studied by the hybrid code method.

Electrons with gyroradii larger than the front width are efficiently accelerated by the first order Fermi mechanism in the vicinity of a collisionless shock wave. However, a non-relativistic electron must have an energy about $m_{\rm p}/m_{\rm e}$ times higher than that of a respective proton to be scattered by MHD waves generated by ions and thus injected into the Fermi acceleration mechanism. That is the problem of electron injection. Being faster, resonant wave–particle interactions usually assume some quasi-linear (small-amplitude) plasma waves. If the local Mach number $\mathscr{M}_{\rm s}$ of the incoming flow in a strong shock wave exceeds $\sqrt{m_{\rm p}/m_{\rm e}}$, the thermal electron distribution becomes highly anisotropic and high frequency whistler type mode generation effects could become important. Levinson (1996) performed a detailed study of resonant electron acceleration by the whistler mode for fast MHD shock waves. The two-stream instability generation of low-hybrid waves was suggested by Laming (2001), Shapiro et al. (2001), and Vaisberg et al. (1983) to model particle acceleration at perpendicular shocks. It was considered by Laming (2001) as the ejecta heating agent for Cas A.

Strong shocks, however, are thought to transfer the ram kinetic energy of the flow into large amplitude nonlinear waves. The thermal electron velocities in the ambient medium are higher than the shock speed if the shock Mach number $\mathscr{M}_{\rm s} < \sqrt{m_{\rm p}/m_{\rm e}}$, allowing for nearly isotropic angular distribution of the electrons. Non-resonant interactions of these electrons with large-amplitude turbulent fluctuations in the shock transition region could result in collisionless heating and pre-acceleration of the electrons (Bykov and Uvarov, 1999). The presence of large-amplitude waves in the shock transition region erodes many of the differences between quasi-parallel and transverse shocks, providing the electron injection mechanism to be similar for these shocks.

An exact modeling of the collisionless shock structure with account of the non-thermal particle acceleration effect requires a non-perturbative self-consistent description of a multi-component and multi-scale system including the strong MHD-turbulence dynamics. That

modeling is not feasible at the moment. We can use, however, some simplified description of a strong shock, with an appropriate parameterization of governing parameters which are: (a) the non-thermal particle diffusion coefficients; (b) the ion injection rate; and (c) the maximum momentum of accelerated particles. Then some predicted observable characteristics of the SNR shocks can be confronted against observational data. We shall discuss first the effects of plasma heating by modified shocks and then some specific predictions for non-thermal emission from SNRs.

2. Plasma heating by collisionless shocks in SNRs

The Alfven Mach number of a shock is determined by

$$\mathscr{M}_{\rm a} = v_{\rm sh}(4\pi\rho_{\rm a})^{1/2}/B \approx 460\ v_{\rm s8}\ n_{\rm a}^{1/2}/B_{-6}, \tag{1}$$

where $n_{\rm a}$ is the ionized ambient gas number density measured in cm^{-3}, B_{-6} is the local magnetic field just before the shock measured in μG and $v_{\rm s8}$ is the shock velocity in 10^8 cm s^{-1}.

The sonic Mach number for a shock propagating in a plasma of the standard abundance is

$$\mathscr{M}_{\rm s} \approx 85\ v_{\rm s8}[T_4(1+f_{\rm ei})]^{-1/2}, \tag{2}$$

where T_4 is the plasma ion temperature measured in 10^4 K and $f_{\rm ei} = T_{\rm e}/T_{\rm i}$. In general, for the processes in the precursor and viscous velocity jump of an MHD collisionless shock wave no equilibration between electrons and ions should be assumed (e.g., Raymond, 2001). Both cases of $f_{\rm ei} \ll 1$ and $f_{\rm ei} > 1$ could be relevant to the SNR systems under consideration. The photoionized gas at the radiative precursor of a fast shock is assumed to have $T_{\rm e} \sim (1\text{–}2) \times 10^4$ K and $f_{\rm ei} \gtrsim 1$. On the other hand, plasma heating due to MHD waves dissipation in the vicinity of the viscous subshock mostly heats the ions, providing $f_{\rm ei} < 1$. It is worth to recall that the plasma parameter $\beta = \mathscr{M}_{\rm a}^2/\mathscr{M}_{\rm s}^2$ is also the ratio of the thermal and magnetic pressures.

The compression ratio and the gas heating in a single-fluid adiabatic quasi-parallel shock of the Mach number $\mathscr{M}_{\rm s}$ are determined by the standard Rankine–Hugoniot relations (e.g., Draine and McKee, 1993)

$$R = \frac{\rho^{(2)}}{\rho^{(1)}} = \frac{(\gamma_{\rm g}+1)\mathscr{M}_{\rm s}^2}{(\gamma_{\rm g}-1)\mathscr{M}_{\rm s}^2+2}, \tag{3}$$

$$\frac{T^{(2)}}{T^{(1)}} = \frac{[2\gamma_{\rm g}\mathscr{M}_{\rm s}^2-(\gamma_{\rm g}-1)][(\gamma_{\rm g}-1)\mathscr{M}_{\rm s}^2+2]}{(\gamma_{\rm g}+1)^2\mathscr{M}_{\rm s}^2}, \tag{4}$$

where $\gamma_{\rm g}$ is the gas adiabatic exponent. For the strong shock limit where $\mathscr{M}_{\rm s} \gg 1$ and $\mathscr{M}_{\rm a} \gg 1$ we have

$$T_{\rm i}^{(2)} \approx 2\frac{(\gamma_{\rm g}-1)}{(\gamma_{\rm g}+1)^2}\mu v_{\rm sh}^2 = 1.38\times 10^7\ v_{\rm s8}^2\ (\mathrm{K}), \tag{5}$$

for any magnetic field inclination. The mass per particle μ was assumed to be $[1.4/2.3]m_{\rm H}$ in the numerical estimation.

3. Plasma heating by CR-modified MHD shocks

However, for the collisionless and radiative shock waves shock relaxation processes are multi-fluid. For strong collisionless shocks in a magnetized plasma the non-thermal particle acceleration effect is expected to be efficient and a significant fraction of the ram pressure could be transferred into the high energy particles (ions only for the non-relativistic shocks). The shock transition of a strong shock of the total Mach number $\mathscr{M}_{\rm s} \gg 1$ is broadened because of the upstream gas deceleration by the non-thermal particle pressure gradient ahead of the viscous gas subshock of the modest Mach number $\mathscr{M}_{\rm sub} \sim 3$ (see for a review Blandford and Eichler, 1987; Jones and Ellison, 1991; Malkov and Drury, 2001).

The total compression ratio $R_{\rm t}$ of a strong MHD shock modified by an efficient non-thermal particle acceleration can be estimated as

$$R_{\rm t} = \frac{\gamma+1}{\gamma-\sqrt{1+2(\gamma^2-1)Q_{\rm esc}/\rho_{\rm a}v_{\rm sh}^3}}, \tag{6}$$

assuming that the energy density in the shock upstream is dominated by the ram pressure and that the CR escape is through the cut-off momentum regime (e.g., Malkov and Drury, 2001). Here, $Q_{\rm esc}$ is the energy flux carried away by escaping non-thermal particles and γ is the effective adiabatic exponent. The distribution function of non-thermal particles and the bulk flow profile in the shock upstream region are sensitive to the total compression ratio $R_{\rm t}$. Thus, the exact calculation of the escape flux $Q_{\rm esc}$ can be performed only in fully nonlinear kinetic simulations. Nevertheless, some approximate iterative approach can be used to make the distribution function consistent with the shock compression. The subshock is the standard gas viscous shock with the compression ratio given by Eq. (3) for $\mathscr{M}_{\rm s} = \mathscr{M}_{\rm sub}$. For that simplified steady state model of a strong CR-modified shock the downstream ion temperature $T_{\rm i}^{(2)}$ can be estimated for the shock of a given velocity if $R_{\rm t}$ and $R_{\rm sub}$ are known:

$$T_{\rm i}^{(2)} \approx \phi(\mathscr{M}_{\rm sub})\frac{\mu v_{\rm sh}^2}{\gamma_{\rm g}R_{\rm t}^2(v_{\rm sh})},$$
$$\text{where } \phi(\mathscr{M}_{\rm sub}) = \frac{2\gamma_{\rm g}\mathscr{M}_{\rm sub}^2-(\gamma_{\rm g}-1)}{(\gamma_{\rm g}-1)\mathscr{M}_{\rm sub}^2+2}. \tag{7}$$

Single fluid strong shock heating represents the limit $\mathscr{M}_{\rm sub} = \mathscr{M}_{\rm s} \gg 1$, since there is no precursor in that case. Using Eq. (3) in the strong shock limit one can see that Eq. (7) reproduces the standard result given by Eq. (5).

The compression ratio $R_t \to (\gamma_g + 1)/(\gamma_g - 1)$ does not depend on the shock velocity in the single-fluid system. This is not the case in the multi-fluid shocks where the total compression ratio depends on the shock velocity and could be higher than that in the single-fluid case. That would imply generally lower post-shock ion temperatures for the strong multi-fluid shock of the same velocity and could be tested observationally.

Consider multi-fluid CR-modified strong shocks. The gas heating mechanism in a CR-modified shock precursor must be specified in the simplified two-fluid approach, providing the connection between the total compression R_t and the gas subshock Mach number $\mathscr{M}_{sub}$.

The gas heating mechanism in the modified shock precursor is still under debate (e.g., Malkov and Drury, 2001) and is usually postulated in shock modeling. There are extensive simulations of the models with *adiabatic heating* of the shock precursor (e.g., Kang et al., 2002). The *Alfven waves dissipation* mechanism was suggested by McKenzie and Völk (1982). The turbulent gas heating due to *acoustic instability wave dissipation* could be more efficient, however, if the acoustic instability develops (e.g., Malkov and Drury, 2001).

The subshock has $\mathscr{M}_{sub} \gtrsim 3$ in the most of the simulated strong shocks with adiabatic heating of the precursor. The result is not too sensitive to the ion injection rate if the rate exceeds some threshold to provide the shock modification by the accelerated ions. The scaling $\mathscr{M}_{sub} \sim 2.9\mathscr{M}_s^{0.13}$ was obtained by Kang et al. (2002). They also found that $R_t \propto \mathscr{M}_s^{3/4}$ is a reasonably good approximation for the two-fluid time-dependent simulations of a CR-modified shock with adiabatic precursor. However, if the precursor heating due to Alfven waves dissipation or the acoustic wave instability is effective then for the plasma compression in the shock precursor could become less efficient.

Notice that the approximations for the shock compression and heating given above were obtained within a simplified two-fluid steady-state approach where the Bohm-like diffusion model was postulated. The possibility of a shock acoustic instability development is still an open question. It requires a dedicated study of the connection between the diffusion coefficient and the local flow parameters. Recent detailed numerical studies of the unsteady CR-modified shocks by Kang et al. (2002) a priori assumed the spatial dependence of the diffusion coefficient $k(p,x) \propto n^{-1}(x)$ to prevent the acoustic instability. The gas heating due to acoustic instability waves or Alfven waves dissipation would change their results.

A very modest heating rate is expected in the case of adiabatic plasma compression in the precursor. That could be the case for very high Alfven Mach number shocks $1 \ll \mathscr{M}_s^2 \ll \mathscr{M}_a$ (i.e., $1 \ll \mathscr{M}_s \ll \sqrt{\beta}$) where the Alfven wave dissipation is not efficient and the acoustic wave instability does not develop. The total compression ratio is $R_t \sim \mathscr{M}_s^{3/4}$ (e.g., Blandford and Eichler, 1987). Then the downstream ion temperature for the case of a weak magnetic field (and $\mathscr{M}_{sub} \sim 3$) can be estimated from:

$$T^{(2)}/T^{(1)} \approx 2.2\sqrt{\mathscr{M}_s}(1 + f_{ei})^{-1}. \quad (8)$$

The latter case of $\mathscr{M}_s \ll \sqrt{\beta}$ is not very realistic for the strong galactic SNR shocks, since that would require the plasma parameter $\beta \gtrsim 100$, while we typically expect $\beta \sim 1$ in the ambient interstellar medium. Note that the same temperature scaling $T^{(2)}/T^{(1)} \propto \sqrt{\mathscr{M}_s}$ is appropriate for strong radiative shocks (see e.g., Bouquet et al., 2000).

Under an assumption that the main heating mechanism of the gas in the precursor region is due to Alfven waves dissipation, a simple asymptotical estimation for the total compression of the shock $R_t \approx 1.5\mathscr{M}_a^{3/8}$ was presented by Berezhko and Ellison (1999). The estimation is valid under the condition of $\mathscr{M}_s^2 \gg \mathscr{M}_a \gg 1$ in the far upstream flow. One may then obtain the ion temperature just behind the strong modified shock with *the preshock heating due to Alfven wave dissipation* (Bykov, 2002) from Eq. (7):

$$T_6^{(2)} \approx 0.32\phi(\mathscr{M}_{sub})v_{s8}^{5/4}n_a^{-3/8}B_{-6}^{3/4}(1 + f_{ei})^{-1}. \quad (9)$$

The ion temperature is measured in 10^6 K. Eq. (9) is valid under the conditions of $\mathscr{M}_s \gg 1$ and $\mathscr{M}_s \gg \sqrt{\beta}$ in the far upstream flow. We have $0.32\phi(3) \approx 1.2$ for $\gamma_g = 5/3$.

An important distinctive feature of the strong CR-modified shock with gas heating by Alfven wave dissipation [given by Eq. (9)] is the dependence of the post-shock temperature on the number density and magnetic field of the incoming plasma $\propto (B/\sqrt{n})^{3/4}$. One may also note a remarkable difference between the single-fluid shock heating given by Eq. (4), where $T^{(2)} \propto v_{sh}^2$ for $\mathscr{M}_s^2 \gg 1$, and those for the CR dominated multi-fluid strong shocks, Eqs. (8) and (9), where $T^{(2)} \propto v_{sh}^a$ with $a \leqslant 1.25$. The predictions are testable with high resolution SNR observations. In case of high enough efficiency of the turbulent heating of gas due to the acoustic instability of a strong shock the index a may exceed 1.25 being closer to the single-fluid limit. That is about the ion temperature. However, the X-ray and multi-wavelength spectra depend in large on the electron distribution.

The initial electron temperature just in the shock downstream depends on the collisionless electron heating (see e.g., Bykov and Uvarov, 1999; Cargill and Papadopoulos, 1988; Laming, 2001). Non-resonant interactions of the electrons with strong non-linear fluctuations generated by kinetic instabilities of the ions in the transition region inside the shock front may play the main role in the heating and pre-acceleration of the electrons, as it was shown in the model by Bykov and Uvarov (1999). They calculated the electron energy

spectrum in the vicinity of the shock waves and showed that the heating and pre-acceleration of the electrons occur on a scale of the order of several hundred ion inertial lengths in the vicinity of the viscous discontinuity. Although the electron distribution function is significantly non-equilibrium near the shock front, its low energy part can be approximated by a Maxwellian distribution. The effective electron temperature just behind the front, obtained in this manner, increases with the shock wave velocity as $T_e \propto v_{sh}^b$ with $b \leqslant 2$. They also showed that if the electron transport in the shock transition region is due to turbulent advection by strong vortex fluctuations on the ion inertial length scale, then the non-resonant electron heating is rather slow (i.e., $b \leqslant 0.5$), but the electrons are still injecting into the diffusive Fermi acceleration. The highly developed vortex-type turbulence is expected to be in the transition regions of very strong shocks. That would imply that the initial $T_e/T_i \propto v_{sh}^{(b-a)}$ just behind the transition region would decrease with the shock velocity for $\mathscr{M}_s \gg 1$.

4. Optical diagnostics of shocked gas

The ratio T_e/T_i in a thin layer (typically $<10^{17}$ cm) just behind a shock can be tested using the optical diagnostics of broad and narrow Balmer lines in the case of a non-radiative shock propagating through *partially ionized* medium (e.g., Chevalier and Raymond, 1978; Raymond, 2001). High resolution *HST* SNR images make that approach very attractive. A simple scaling $T_e/T_i \propto v_{sh}^{-1}$ was obtained by Ghavamian et al. (2001) from optical observations of SN1006, Tycho, Kepler, RCW86, and Cygnus Loop. The scaling is generally consistent with the interplanetary shock data compiled by Schwartz et al. (1988). The degree of electron–ion equilibration in collisionless shock is found to be a declining function of shock speed. In the case of strong vortex-type turbulence in the shock transition region $(a-b) \sim 1$ is generally consistent with the Alfven heating case described.

It is worth to have in mind, however, that the effect of non-thermal particle acceleration on the total compression ratio of a non-radiative shock propagating through a *partially ionized* medium could be lower than that in a fully ionized ambient gas. The reason is that MHD wave damping in the partially ionized far upstream region limits maximal energies of accelerated particles. The limits imposed on the diffusive shock acceleration of particles due to ion-neutral MHD wave damping have been discussed by Drury et al. (1996). They considered the spectra of Alfven waves driven by instabilities of shock accelerated ions in a partially ionized plasma and obtained the upper cut-off energy of a proton due to ion-neutral wave damping as

$$E_m \leqslant v_{s7}^3 T_4^{-0.4} n_n^{-1} n_i^{0.5} \mathscr{P}_{-1}^{CR} \text{ GeV}, \quad (10)$$

where n_n is the neutral particle density, n_i is the ion density (both are measured in cm^{-3}), and $\mathscr{P}_{-1}^{CR}$ is the total particle pressure normalized to 10% of the shock ram pressure. That results in a reduction of the energy flux carried away by escaping non-thermal particles as given by Eq. (6) if the particle injection rate is the same. The value Q_{esc} depends on the cut-off energy of escaping fast particles which is lower in partially ionized media. Since the cut-off energy $E_m \propto v_{sh}^3$ one may expect that a strong shock of a velocity $\gtrsim 100$ km s^{-1} (e.g., Cygnus Loop SNR) would have the compression ratio and the mean post-shock temperature close to that given by the Rankine–Hugoniot relations Eq. (5), while faster shocks of $\gtrsim$1000 km s^{-1} (SN1006, Tycho) could be strongly CR-modified and might have reduced mean temperatures.

The electron and ion temperatures eventually equilibrate in the much thicker post-shock layer due to Coulomb collisions. The complete e–i Coulomb equilibration requires the system age $t \gtrsim 10^{10}\ T_6^{3/2}/n(s)$, where the post-shock density n is measured in cm^{-3} (see e.g., Mewe, 1990 for a review). A natural way to study the heating of the post-shock gas in SNRs is X-ray observations.

5. X-ray emission of shocked gas

Early SNR X-ray observations were used to constrain the electron temperatures behind the strong shocks. It is not an easy task, however, to derive a reliable estimation of the shocked gas temperature from spatially unresolved SNR spectra. Hot gas behind the blast wave, heated ejecta material of a complex morphology, emission of energetic non-thermal particles (bremsstrahlung, synchrotron, and inverse Compton) and compact objects (e.g., pulsar wind nebula) altogether contribute to an unresolved SNR spectrum. Modern X-ray telescopes aboard *Chandra* and *XMM-Newton* provide high quality images of SNRs and high resolution spectra up to 10 keV. That allows studies of a few arcsecond scale structures in SNRs. With that high resolution observations of galactic SNRs it is possible to distinguish the contributions of shocked ambient gas behind the blast wave from that of the shocked ejecta material.

High resolution observations of Cas A have been recently performed with *Chandra* by Gotthelf et al. (2001) and *XMM-Newton* by Bleeker et al. (2001) and Willingale et al. (2002). The observations revealed the forward shock with a thin wisp of X-ray emission likely due to shocked interstellar gas of estimated temperature $T = 2.0 \pm 0.5$ keV ($nt \leqslant 10^{10.8\pm0.2}$ cm^{-3} s) with an additional hard component (Gotthelf et al., 2001). The forward shock velocity estimation 3500–4500 km s^{-1} was

given by Willingale et al. (2002). For a low electron equilibration case ($f_{ei} \lesssim 0.1$) the derived temperature is consistent with gas heating by a shock of a compression ratio $R_t \approx 4$ (a single-fluid or a CR-modified shock with acoustic instability heating). The case of a CR-modified shock with Alfven wave dissipation propagating through an ambient medium of $n \sim 0.1$ cm^{-3} and magnetic field $B \gtrsim 3$ μG would be consistent with the Cas A data if a moderate electron equilibration ($f_{ei} \sim 0.3$) is allowed. A CR modified shock with adiabatic gas heating in the precursor is not consistent with the Cas A data which is not surprising since $\mathscr{M}_s \gg \sqrt{\beta}$. The *Chandra* spectrum of the outer rim of Cas A studied by Gotthelf et al. (2001) is dominated by power-law emission component. Synchrotron emission of shock accelerated electrons could contribute there as it is believed to be the case in SN1006 (Koyama et al., 1995; Reynolds, 1998). For Cas A, however, no direct radio counterpart has been found by Gotthelf et al. (2001) making the synchrotron contribution somewhat problematic. Moreover, the *XMM-Newton* study of hard X-ray continuum of Cas A by Bleeker et al. (2001) found that the hard emission is spread over the whole remnant. Bremsstrahlung emission of accelerated electrons was considered as a possible mechanism for the hard emission origin. The non-thermal bremsstrahlung origin of Cas A hard emission requires an energy input of $\sim 10^{40}$ erg s^{-1} (e.g., Laming, 2001). Magnetic reconnection effects inside the remnant can play a role in the origin of that hard X-ray emission component.

There is a possible evidence for a CR-modified shock in X-ray data. *Chandra* observations of 1E0102.2-7219 a SNR in the Small Magellanic Cloud by Hughes et al. (2000) revealed a low gas temperature ($\lesssim$ keV) behind the forward shock wave of estimated velocity ~6000 km s^{-1}. The observations could be understood if a significant fraction of the shock ram energy went into cosmic rays (Decourchelle et al., 2000; Hughes et al., 2000). A keV-regime ion temperature is expected behind the shock of ~6000 km s^{-1} from Eq. (9) assuming a μG scale ambient magnetic field. If confirmed, that would provide an interesting case of a multi-fluid SNR shock.

A few arcsecond angular resolution attainable with *Chandra* and *XMM-Newton* telescopes allows a spectral study of fast moving supernova ejecta fragments. They were first discovered long ago as a fast moving optical and radio knots in Cas A. A distinctive feature of the optical knots in Cas A was their high enrichment with oxygen and some other SN nucleosynthesis products (e.g., Chevalier and Kirshner, 1978).

6. X-ray line emission of supernova ejecta fragments

X-ray knots were discovered with *ROSAT* in the Vela SNR by Aschenbach et al. (1995) as 'shrapnels', boomerang structures outside of the main shell. High-resolution *Chandra* observations of shrapnel A reported by Miyata et al. (2001) revealed a head-tail structure of the apparent size $8'.4 \times 4'.1$ (0.6×0.3 pc at 250 pc distance). They estimated the gas pressure in the head to be roughly 10 times higher than that in the tail and $T_e \sim 0.5$ keV. The oxygen abundance was $0.34^{+0.12}_{-0.08}$ of the solar value, while that of Si was estimated as 3^{+2}_{-1} times of the solar.

Clumpy structure of X-ray line emission is rather a common feature of high resolution SNR observations. Willingale et al. (2002) found an emission component in Cas A that is probably due to heating of ejecta clumps sweeping up the ambient gas. They also note that the observed Fe–K line emission is confined to two large clumps. A localized region of 6.4 keV emission indicating the presence of Fe XVII or lower ionization states was found in the supernova remnant RCW 86 with *ASCA* instrument by Vink et al. (1997). The clumpy emission structure is also seen in the *XMM-Newton* images of Tycho (Decourchelle et al., 2001).

Fast moving isolated fragments of a supernova ejecta composed of heavy elements should be sources of K_α X-ray line emission of the nuclear-processed products of the SN. Supersonic motion of the knots in the intercloud medium results in a bow-shock/knot-shock structure creation. Fast non-thermal particles accelerated by Fermi mechanism in the MHD collisionless shocks diffuse through a cold metallic knot, suffering from Coulomb losses and producing the X-ray emission. The X-ray emission from fast moving knots of masses $M_k \leqslant 10^{-2} M_\odot$, containing $M_i \leqslant 10^{-3} M_\odot$ of any metal impurities like Si, S, Ar, Ca, Fe was modeled by Bykov (2002). The distribution of accelerated electrons was simulated using a kinetic description of charged particles interacting with strong CR-modified MHD shock. Nonlinear effects of shock modification by the non-thermal particles pressure were accounted for. There are a number of predictions of the model.

Energetic (MeV-regime) particles accelerated at the fragment bow shock have high penetrating ability and irradiate both hot gas and cold metal rich matter of the fragment. A wide range of ionization states of K-shell line emitting ions is resulting and it cannot be reproduced by thermal plasma. In particular, the 6.4 keV iron line emission is expected from SN fragments interacting with molecular clouds, and may account for "iron line clumps" recently observed with *Chandra* in the Galactic Center region by Bamba et al. (2002). Another possible source of the 6.4 keV iron line emission is a molecular cloud irradiated by a powerful hard X-ray source producing fluorescent X-ray lines as an X-ray reflection nebula (Sunyaev et al., 1993).

The K_α line emission is most prominent for the knots propagating through dense molecular clouds. In that case the X-ray line spectrum of an ejecta fragment is

dominated by the low ionization states of the ions. For instance, the line emission was simulated for a fast ($v_k \gtrsim 1000$ km s^{-1}) compact knot of a radius $R \sim 3 \times 10^{16}$ cm and mass $M_k \sim 10^{-3} M_\odot$, containing $M_{Fe} \sim 10^{-4} M_\odot$. The knot was propagating through a molecular cloud of a density $n_a \approx 10^3$ cm^{-3}. The simulated metal line luminosities are $L_x \gtrsim 10^{31}$ erg s^{-1}. High resolution *XMM-Newton* and *Chandra* observations are able to detect the K_α and K_β line emission from the knots at distances up to a few kpcs. The bow shock of a fragment propagating through a dense cloud should be a radiative wave with prominent infrared and optical emission. The lifetime of such a knot in a molecular cloud (~100 years) is rather short.

The knots propagating through tenuous interstellar matter are of a lower surface brightness, but long-lived. X-ray line spectra with higher ionization states of the ions are expected in that case.

A fast fragment of a scale $\gtrsim 10^{17}$ cm and of the mass $10^{-3} M_\odot$, entering a molecular clump will have $\rho_a/\rho_k \gtrsim 1$ and a strong shock would be driven into the metal-rich fragment. Ion acceleration time to $\lesssim 100$ MeV/nucl at the strong internal shock of ejecta fragment would be below a year. The composition of the accelerated ions must be highly metal-rich. Such a fragment should be a source of γ-ray lines and a source also of light and other elements of a spallogenic origin produced by accelerated ion interactions with the metal-rich knot. It would be seen as a bright transient source. γ-ray line sources of $L_\gamma \lesssim 10^{34}$ erg s^{-1} could be observed from nearby molecular clouds with SN activity (e.g., Vela, Orion, etc.). An ensemble of unresolved sources from dense molecular clouds in the central regions of the Galaxy could contribute to diffuse γ-ray line emission. There is an evidence for some broad spectral excesses found by *GRO COMPTEL* in the galactic inner radian (Bloemen et al., 1997). Forthcoming *INTEGRAL* observations of diffuse emission would help to resolve the issue.

Optical depth effect due to resonant scattering is important for K-shell lines. Compact dense knots could be opaque for some X-ray lines and that is important for the interpretation of their abundances. In the case of the Vela fragment A, the *Chandra* line spectrum obtained by Miyata et al. (2001) can be reproduced in the model where the optical depth effect is taken into account for an oxygen dominated fragment of a mass $\sim 10^{-2} M_\odot$, containing about $\sim 10^{-3} M_\odot$ of silicon (Bykov, 2002).

There are a number of factors limiting the fast ejecta fragment lifetime. A fast moving knot is decelerating due to the interaction with the ambient gas. The deceleration time of a knot of velocity v_k and radius R_k can be estimated as $\tau_d \sim M_k/(\rho_a v_k \pi R_k^2)$. The knot hydrodynamical crushing effects could have shorter timescale, of the order of time for an internal shock to cross the knot. However, if a significant fraction of a knot bow shock ram pressure is transferred to high energy particles the post-shock gas pressure drops down $\propto R_t^{-1}(v_{sh})$. The internal shock is slower in that case and the knot stability conditions are affected also. That is especially important for the lifetime estimations of fast knots propagating through a rarefied ambient medium. The Vela shrapnel A has a lifetime of about 10^4 years consistent with the deceleration time of an ejecta fragment of 0.3 pc scale and $M_k \sim 10^{-2} M_\odot$, propagating through an ambient medium of a density ~0.1 cm^{-3}. A SN fragment could have even longer lifetime of $\gtrsim 10^5$ years in a tenuous interstellar medium of a density $\lesssim 0.01$ cm^{-3}. Assuming the SN rate about 0.03 yr^{-1} for the Milky Way one may expect an instantaneous contribution from the ensemble of numerous fast moving fragments of ~3000 SNe in the rarefied medium.

The ensemble of unresolved SN ejecta fragments could provide a diffuse iron line luminosity $L_x \gtrsim 10^{36}$ erg s^{-1}. The X-ray lines contributed by fast SN ejecta fragments to the galactic ridge emission are broad because of rather high fragment velocities $v_k \gtrsim 10^3$ km s^{-1}. Analysis of *ASCA* observations of the Galactic ridge emission by Tanaka (2002) revealed broad He-like and H-like iron K-lines, corresponding to a velocity dispersion of a few thousand km s^{-1}.

7. Non-thermal emission of SNRs in molecular cloud

Massive stars that are the likely progenitors of core collapsed supernovae are expected to be spatially correlated with molecular clouds. An interaction of a SNR with a molecular cloud is expected to manifest itself by a number of spectacular appearances in a wide range of wavelengths from radio to γ-rays.

Non-thermal emission from an SNR is a signature of the presence of accelerated particles that has important implications to the cosmic ray origin problem. Substantial efforts to detect γ-ray emission of cosmic rays from SNRs have been undertaken by *Compton GRO*. *EGRET CGRO* has detected four extended γ-ray sources (Esposito et al., 1996) that are candidates to be identified with SNRs (IC443, γ-Cyg, W28, W44), though some of many unidentified *EGRET sources* might be as well related to SNRs. The remnants that are likely candidates to be γ-ray sources in *CGRO EGRET observations* show evidences for interaction with molecular gas. Positive excesses of both 3–10 and 10–30 MeV-regimes emission were found recently on the IC 443 position by Bronsveld et al. (2002). They analyzed *CGRO COMPTEL* deep exposure of the Galactic Anti-Centre region. The significance of the apparent excesses depends on the Galactic diffuse emission model and it is reaching more than 3σ for 3–10 MeV-regime. The GeV regime *CGRO EGRET* spectrum of index ~2.0, if extrapolated down to about 3 MeV, appears to be consistent with the *CGRO COMPTEL* data (Bronsveld et al., 2002). Upper limits

from *CGRO OSSE* observations reported by Sturner et al. (1997) also constrain the emission below MeV-regime.

When γ-ray emission was apparently detected from SNRs by *CGRO*, it was realized that the γ-ray spectrum could not be fitted by a pure pion decay spectrum and some other component was needed (Esposito et al., 1996; Gaisser et al., 1998; Sturner et al., 1997). In addition to the pion decays (see e.g., Drury et al., 1994), the relevant processes are bremsstrahlung emission of relativistic electrons and inverse Compton emission. Gaisser et al. (1998) modeled these processes in detail in order to fit the observed γ-ray spectra of the remnants IC 443 and γ-Cygni. They assumed acceleration to a power law spectrum in the shock front and determined the spectral index, electron to proton ratio, and the upper energy cutoff.

The evolution of the relativistic component in a supernova remnant has been modeled by a number of groups. They used Sedov–Taylor adiabatic shock dynamics in a homogeneous medium. Sturner et al. (1997) assumed particle acceleration in the shock front with an E^{-2} energy spectrum and followed the evolution of the particle spectrum. They modeled non-thermal emission from IC 443 as synchrotron emission in the radio and bremsstrahlung in γ-rays. de Jager and Mastichiadis (1997) dealt with the same processes in W44, as well as inverse Compton emission. They noted that the observed radio spectrum is flatter than would be expected from shock acceleration of newly injected particles and suggested that the particles originated from a pulsar in the supernova remnant. Baring et al. (1999) presented calculations of the broad-band emission from non-linear shock models of shell-type SNRs. They used a Monte Carlo simulation of the particle acceleration taking into account the non-linear shock structure.

Observations of the optical/IR emission spectra of IC 443 indicate the presence of radiative shock and a different model is needed. Hydrodynamical modeling of a SNR interacting with a molecular cloud has been recently performed by Chevalier (1999). The remnants evolve in the inter-clump medium of a molecular cloud. The non-thermal multi-wavelength spectrum of a SNR interacting with a molecular cloud was studied by Bykov et al. (2000). To simulate the spectra of non-thermal electrons in the SNR shell they solved a kinetic equation for the distribution function of the electrons, accounting for injection, diffusive transport, advection, the first and the second order Fermi acceleration and synchrotron and the Coulomb losses. There are three zones in the inhomogeneous model: the pre-shock region, the shock transition region, and the post-shock flow, from where most of the non-thermal emission of shock-accelerated particles originates.

The propagation of a radiative shock wave through a molecular cloud leads to a substantial non-thermal emission both in hard X-rays and in γ-rays. The complex structure of a molecular cloud consisting of dense massive clumps embedded in the interclump medium could result in localized sources of hard X-ray/γ-ray emission correlated with both bright molecular emission (Bykov et al., 2000). It has been shown that hard X-ray and γ-ray emission structure should consist of an extended shell-like structure (appearing also in radio as a shell of relatively flat spectrum) related to the radiative shock and localized sources corresponding to shocked molecular clumps. The

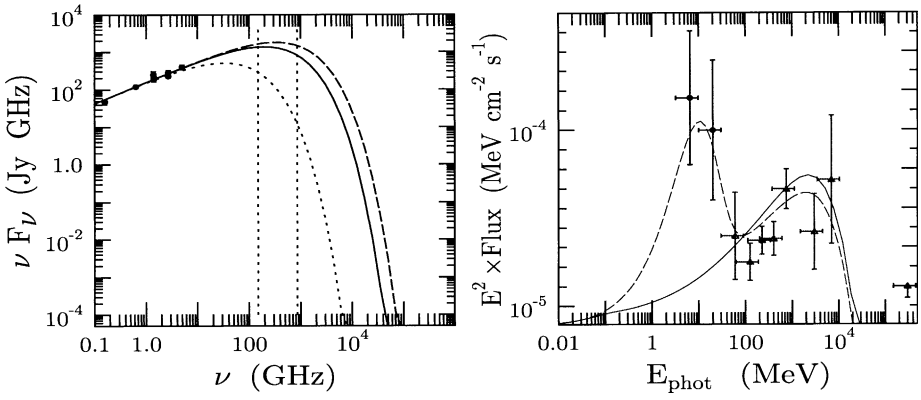

Fig. 1. Broadband νF_ν spectrum of the shell of IC 443 (distance 1.5 kpc) calculated from a model of non-thermal electron production by a radiative shock by Bykov et al. (2000). The shock velocity is 150 km s^{-1}, the interclump number density is 25 cm^{-3}. *Left panel*: The simulated radio synchrotron spectra are given for different possible values of the magnetic field in the radiative shell. The magnetic field values are 100, 60 and 6 μG from the top to the bottom curves. Radio observations data of IC 443 on the left panel are from Erickson and Mahoney (1985). We indicated also the frequency band where submillimetre polarimetric observations of the shell with the *SCUBA* camera of the *JCMT* are possible. *Right panel*: Solid and dashed curves are corresponding to different possible values of the stochastic Fermi acceleration in the post-shock region. *COMPTEL* data on IC 443 (for low background model) are taken from Bronsveld et al. (2002). The observational data points are from Esposito et al. (1996) for the *EGRET* source 3EG J0617+2238. Upper limits for γ-rays $\geqslant$ 300 GeV are from *Whipple* observations of IC 443 by Buckley et al. (1998).

shocked clumps would have a (sub)parsec scales and emit very hard X-ray continuum spectra. Potential candidate sources were found in IC443 (Bocchino and Bykov, 2003) and in γ-Cygni (Uchiyama et al., 2002). High resolution spectra are required, however, to distinguish between the shocked clump and fast moving ejecta fragments discussed above.

The extended shell of IC443 has been well studied in radiowaves since the 1960s (e.g., Erickson and Mahoney, 1985). Relativistic electrons responsible for the observed synchrotron radio emission of the shell can be accelerated by the forward shock and produce substantial γ-ray emission with photon energies above MeV. It has been shown by Bykov et al. (2000) that the γ-ray emission above 100 MeV observed by *EGRET* is consistent with that of relativistic bremsstrahlung of the radio-emitting electrons (see the right panel of Fig. 1). The spectrum of γ-ray emission of the shell depends also on the second order Fermi acceleration by MHD turbulence in the post-shock layer. That is illustrated on the right panel of Fig. 1 where two curves correspond to two possible regimes of stochastic acceleration. In that respect MeV-regime emission is crucial to distinguish between physically plausible models of particle acceleration by radiative shocks. The MeV-regime continuum emission is most likely produced by an energetic leptons (bremsstrahlung or an extended inverse Compton components). Thus, the MeV spectrum could help to estimate the leptonic contribution to higher energies constraining the nucleonic component of SNR energetic particles.

In the case of IC 443 there are a number of sources potentially contributing to the observed γ-ray emission. These are: the SN extended shell seen in the radio, the pulsar wind nebula with hard core emission appeared in the *XMM-Newton* spectrum (Bocchino and Bykov, 2001), shocked clumps and molecular gas irradiated by accelerated particles. Maximum-likelihood analysis of the *EGRET* data must account for all the possible contributions but not just for a single point-like source pattern. That analysis is necessary to constrain the leptonic and nucleonic energetic particle components. It would require a few arcmin scale angular resolution. Hard X-ray and γ-ray observations of the sources with *INTEGRAL* and *GLAST* would help to resolve the contributions.

Acknowledgements

I am very grateful to W. Hermsen and W. Becker for the very interesting meeting and to SRON and COSPAR for travel support. The work was supported by INTAS/ESA 99-1627 and RBRF 01-02-16654 and 03-02-17433 grants.

References

Aschenbach, B., Egger, R., Trümper, J. Discovery of explosion fragments outside the Vela supernova remnant shock-wave boundary. Nature 373, 587–588, 1995.

Bamba, A., Murakami, H., Senda, A. et al., Diffuse X-rays in the Galactic Center Region – the zoo of iron line clumps, non-thermal filaments and hot Plasmas. Available from <astro-ph/0202010> 2002.

Baring, M.G., Ellison, D.C., Reynolds, S.P., et al. Radio to γ-ray emission from shell-type supernova remnants: predictions from non-linear shock acceleration models. Astrophys. J. 513, 311–338, 1999.

Berezhko, E.G., Ellison, D.C. A simple model of non-linear diffusive shock acceleration. Astrophys. J. 526, 385–399, 1999.

Blandford, R., Eichler, D. Particle acceleration at astrophysical shocks: a theory of cosmic ray origin. Phys. Rep. 154, 1–75, 1987.

Bleeker, J.A.M., Willingale, R., van der Heyden, K.J., et al. Cas A: on the origin of the hard X-ray continuum and the implication of the observed OVIII Ly-α/Ly-β distribution. Astron. Astrophys. 365, L225–L231, 2001.

Bloemen, H., Bykov, A.M., Diehl, R., et al. COMPTEL spectral study of the inner Galaxy, in: AIP Conference Proceedings. vol. 410, pp. 1074–1079, 1997.

Bocchino, F., Bykov, A.M. The plerion nebula in IC443: the XMM-Newton view. Astron. Astrophys. 376, 248–253, 2001.

Bocchino, F., Bykov, A.M. XMM-Newton study of hard X-ray sources in IC443. Astron. Astrophys. 400, 203–211, 2003.

Bouquet, S., Teyssier, R., Chieze, J.P. Analytical study and structure of a stationary radiative shock. Astrophys. J. Suppl. 127, 245–252, 2000.

Bronsveld, P., Hermsen, W., Kuiper L., et al. A deep study of compact sources in the Galactic Anti-Centre with COMPTEL, in: Goldwurm, A., Neumann, D., Tran Thanh, J. (Eds.), The XXII Moriond Astrophysics Meeting "The γ-Ray Universe". pp. 113–118, 2002.

Buckley, J.H., Akerlof, C.W., Carter-Lewis, D.A., et al. Constraints on cosmic ray origin from TeV γ-ray observations of supernova remnants. Astron. Astrophys. 329, 639–658, 1998.

Bykov, A.M., Uvarov, Yu.A. Electron kinetics in collisionless shock waves. JETP 88, 465–475, 1999.

Bykov, A.M., Chevalier, R.A., Ellison, D.C., et al. Non-thermal emission from a supernova remnant in a molecular cloud. Astrophys. J. 538, 203–216, 2000.

Bykov, A.M. X-ray line emission from supernova ejecta fragments. Astron. Astrophys. 390, 327–335, 2002.

Cargill, P.J., Papadopoulos, K. A mechanism for strong shock electron heating in supernova remnants. Astrophys. J. 329, L29–L32, 1988.

Chevalier, R.A., Kirshner, R.P. Spectra of Cassiopeia A. II. Astrophys. J. 219, 931–941, 1978.

Chevalier, R.A., Raymond, J.C. Optical emission from a fast shock wave – the remnants of Tycho's supernova and SN 1006. Astrophys. J. 225, L27–L30, 1978.

Chevalier, R.A. Supernova remnants in molecular clouds. Astrophys. J. 511, 798–811, 1999.

Decourchelle, A., Ellison, D.C., Ballet, J. Thermal X-ray emission and cosmic ray production in supernova remnants. Astrophys. J. 543, L57–L60, 2000.

Decourchelle, A., Sauvageot, J.L., Audard, M., et al. XMM-Newton observation of the Tycho supernova remnant. Astron. Astrophys. 365, L218–L224, 2001.

de Jager, O., Mastichiadis, A. A relativistic bremsstrahlung/inverse Compton origin for 2EG J1857+0118 associated with supernova remnant W44. Astrophys. J. 482, 874–880, 1997.

Draine, B.T., McKee, C.F. Theory of interstellar shocks. Ann. Rev. Astron. Astrophys. 31, 373–432, 1993.

Drury, L.O'C., Aharonian, F.A., Völk, H.J. The γ-ray visibility of supernova remnants. A test of cosmic ray origin. Astron. Astrophys. 287, 959–971, 1994.

Drury, L.O'C., Duffy, P., Kirk, J.G. Limits on diffusive shock acceleration in dense and incompletely ionised media. Astron. Astrophys. 309, 1002–1010, 1996.

Erickson, W.C., Mahoney, M.J. Clark Lake observations of IC 443 and Puppis A. Astrophys. J. 290, 596–601, 1985.

Esposito, J.A., Hunter, S.B., Kanbach, G., et al. EGRET observations of radio-bright supernova remnants. Astrophys. J. 461, 820–827, 1996.

Gaisser, T.K., Protheroe, R.J., Stanev, T. γ-ray production in supernova remnants. Astrophys. J. 492, 219–234, 1998.

Ghavamian, P., Raymond, J., Smith, R.C., et al. Balmer-dominated spectra of non-radiative shocks in the Cygnus Loop, RCW 86, and Tycho supernova remnants. Astrophys. J. 547, 995–1009, 2001.

Gotthelf, E.V., Koralesky, B., Rudnick, L., et al. Chandra detection of forward and reverse shocks in Cas A. Astrophys. J. 552, L39–L43, 2001.

Hughes, J.P., Rakovski, C.E., Decourchelle, A. Electron heating and cosmic rays at a supernova shock from Chandra X-ray observations of 1E0102.2-7219. Astrophys. J. 543, L61–L65, 2000.

Jones, F.C., Ellison, D.C. The plasma physics of shock acceleration. Space Sci. Rev. 58, 259–346, 1991.

Kan, J.R., Lyu, L.H., Mandt, M.E. Quasi-parallel collisionless shocks. Space Sci. Rev. 57, 201–236, 1991.

Kang, H., Jones, T.W., Gieseler, U.D.J. Numerical studies of cosmic-ray injection and acceleration. Astrophys. J. 579, 337–358, 2002.

Kennel, C.F., Edmiston, J.P., Hada, T. A quarter century of collisionless shock research, in: Stone, R.G., Tsurutani, B.T. (Eds.), Collisionless Shocks in Heliosphere: A Tutorial Review. AGU, Washington, DC, pp. 1–36, 1985.

Koyama, K., Petre, R., Gotthelf, E.V., et al. Evidence for shock acceleration of high-energy electrons in the supernova remnant SN1006. Nature 378, 255–258, 1995.

Krauss-Varban, D. Waves associated with quasi-parallel shocks: generation, mode conversion and implications. Adv. Space Res. 15 (8/9), 271–284, 1995.

Laming, J.M. Accelerated electrons in Cassiopeia A: thermal and electromagnetic effects. Astrophys. J. 563, 828–841, 2001.

Levinson, A. On the injection of electrons in oblique shocks. MNRAS 278, 1018–1024, 1996.

Malkov, M.A., Drury, L.O'C. Non-linear theory of diffusive acceleration of particles by shock waves. Rep. Prog. Phys. 64, 429–481, 2001.

McKenzie, J.F., Völk, H.J. Non-linear theory of cosmic ray shocks including self-generated Alfven-Waves. Astron. Astrophys. 116, 191–200, 1982.

Mewe, R. Ionization of hot plasmas, in: Brinkmann, W. (Ed.), Physical Processes in Hot Cosmic Plasmas. Kluwer Academic Publishers, Dordrecht, pp. 39–64, 1990.

Miyata, E., Tsunemi, H., Aschenbach, B., Mori, K. Chandra X-ray observatory study of Vela shrapnel A. Astrophys. J. 559, L45–L48, 2001.

Quest, K.B. Theory and simulations of collisionless parallel shocks. J. Geophys. Res. 93, 9649–9666, 1988.

Raymond, J.C. Optical and UV diagnostics of supernova remnant shocks. Space Sci. Rev. 99, 209–218, 2001.

Reynolds, S.P. Models of synchrotron X-Rays from shell supernova remnants. Astrophys. J. 493, 375–386, 1998.

Schwartz, S.J., Thomsen, M.F., Bame, S.J., et al. Electron heating and the potential jump across fast mode shocks. J. Geophys. Res. 93, 12923–12931, 1988.

Shapiro, V.D., Lee, M.A., Quest, K.B. Role of lower hybrid turbulence in surfing acceleration at perpendicular shocks. J. Geophys. Res. 106, 25023–25030, 2001.

Sturner, S.J., Skibo, J.G., Dermer, C.D., et al. Temporal evolution of non-thermal spectra from supernova remnants. Astrophys. J. 407, 606–610, 1997.

Sunyaev, R.A., Markevitch, M., Pavlinsky, M. The center of the Galaxy in the recent past – a view from GRANAT. Astrophys. J. 490, 619–632, 1993.

Tanaka, Y. ASCA observation of X-ray emission from the galactic ridge. Astron. Astrophys. 382, 1052–1060, 2002.

Tsurutani, B.T., Lin, R.P. Acceleration of >47 and >2 keV electrons by interplanetary shocks at 1 AU. J. Geophys. Res. 90, 1–11, 1985.

Uchiyama, Y., Takahashi, T., Aharonian, F.A., et al. ASCA view of the supernova remnant γ-Cygni: bremsstrahlung X-ray spectrum from loss-flatened electron distribution. Astrophys. J. 571, 866–875, 2002.

Vaisberg, O.L., Galeev, A.A., Zastenker, G.N., et al. Electron heating at a front of a strong collisionless shock wave. JETP 58, 716–720, 1983.

Vink, J., Kaastra, J., Bleeker, J.A.M. X-ray spectroscopy of the supernova remnant RCW 86. Astron. Astrophys. 328, 628–633, 1997.

Willingale, R., Bleeker, J.A.M., van der Heyden, K.J., Kaastra, J.S., Vink, J. X-ray spectral imaging and Doppler mapping of Cas A. Astron. Astrophys. 381, 1039–1048, 2002.